Variational Objective Analysis for Atmospheric Field Programs: A Model Assessment

D. E. WALISER
Institute for Terrestrial and Planetary Atmospheres, State University of New York, Stony Brook, New York

J. A. RIDOUT
Marine Meteorology Division, Naval Research Laboratory, Monterey, California

S. XIE
Lawrence Livermore National Laboratory, Livermore, California

M. ZHANG
Institute for Terrestrial and Planetary Atmospheres, State University of New York, Stony Brook, New York

(Manuscript received 5 December 2001, in final form 23 May 2002)

ABSTRACT

The objective of this study is to examine the effectiveness of the variational objective analysis (VOA) for producing realistic diagnoses of atmospheric field program data. Simulations from the Naval Research Laboratory's Coupled Ocean/Atmosphere Mesoscale Prediction System (COAMPS) were sampled in a manner consistent with a typical field program using idealized sounding arrays and, surface and top of the atmosphere flux information. These data were then subject to a conventional form of analysis in which only a mass constraint was applied, hereafter referred to as the reference analysis, as well as to the complete VOA procedure. The diagnosed results from both analyses were then compared to time- and domain-averaged quantities from the model.

The results showed that for diagnosed vertical velocity and vertical advective tendencies, the VOA values typically exhibited considerably smaller errors compared to the values from the reference analyses, with the level of improvement and overall accuracy being dependent on synoptic and sampling conditions. The improvements tend to be greatest during disturbed conditions, with the errors typically being smaller and comparable between the two analyses during undisturbed conditions. The errors for both analyses increase as the spatial domain decreases and for the most part decrease with more frequent temporal sampling. However, the improvement achieved by having more frequent sampling is rather modest for the VOA since it already incorporates time-mean surface and TOA fluxes as constraints and thus indirectly incorporates some aspects of the variability between soundings. Highly relevant is the finding that overall the errors in vertical velocity and vertical advective tendencies from the reference analyses have a magnitude similar to, or greater than, the variability of the field being diagnosed, whereas the errors in these quantities from the VOA are typically less than the variability of the field. The analysis also showed no obvious systematic level-by-level improvement gained by the VOA analysis over the reference analysis in diagnosing the horizontal moisture flux convergence, mass divergence, or horizontal advective tendencies, notwithstanding the VOA's application of column-integrated constraints of mass, moisture, heat, and momentum conservation.

Additional soundings were found to be more beneficial to the reference analyses than the VOA analyses and in some cases allowed the error characteristics of the reference analysis to become similar to those of the VOA analysis. Noteworthy is the finding that the results from the VOA analyses using five soundings were often as good or better than the results from the reference analyses using nine soundings. The impact that hydrometeor measurements would have in providing additional constraints on the VOA was also investigated. The impact was found to be mostly negligible when averaging over relatively large space scales or timescales. On the other hand, for frequent sampling (e.g., 1–3 h) and small spatial scales (i.e., $<\sim$100 km), there is a definite favorable impact on the VOA results for highly disturbed periods. The implications that the above results have on conducting atmospheric field programs and analyzing their results are discussed.

1. Introduction

The goal of most atmospheric field programs has been to provide, to the extent possible, a complete description of the variability of the atmosphere within a fairly localized region during one or more ''intensive observation periods'' (IOPs), each of which may extend over a number of days to months. Examples of such field programs include the Barbados Oceanographic and Meteorological Experiment (BOMEX; Holland and Rasmusson 1973; Nitta and Esbensen 1974), the Global Atmosphere Research Program (GARP) Atlantic Tropical Experiment (GATE; ISMGG 1974), the Australian Monsoon Experiment (AMEX; Gunn et al. 1989), the Severe Environmental Storm and Mesoscale Experiment

Corresponding author address: Duane E. Waliser, Institute for Terrestrial and Planetary Atmospheres, Endeavour Hall #205, State University of New York, Stony Brook, NY 11794-5000.
E-mail: duane.waliser@sunysb.edu

(SESAME; Kuo and Anthes 1984; Carney and Vincent 1986), the Coupled Ocean–Atmosphere Response Experiment (COARE; Webster and Lukas 1992), and the Atmospheric Radiation Measurement (ARM) program (Stokes and Schwartz 1994). In each of these field experiments, atmospheric observations were gathered with a greater temporal and spatial sampling than what would have been typically provided by the synoptic weather network. In addition, the observing systems associated with these field programs were often augmented by state-of-the-art instrumentation that provided measurements of quantities not usually or not well observed by the available operational network.

Once the field program data are gathered they are typically used for atmospheric budget analysis, process studies, and as large-scale forcing to drive single-column model (SCM; e.g., Randall et al. 1996; Ghan et al. 2000) or cloud-resolving model (CRM) simulations as a means to develop and evaluate physical parameterizations (e.g., clouds, convection). However, before the data can be fully exploited, it must be subjected to objective analysis techniques in order to account for the sampling errors that arise from measurement error or missing data, as well as to remove small-scale variability that aliases into the desired timescales and space scales. Having a robust form of this analysis is crucial since the diagnosis of important unmeasured quantities, such as vertical velocity, advective tendencies, convective transports, and latent heating, necessarily rely on derivatives of the measured quantities and in some cases integrals of these derivatives. Thus, relatively small errors in the measured quantities can have a significant impact on the final results of the analysis, particularly on the diagnosed quantities. Given that there has often been very little to constrain the subjective, and even the objective, aspects of these procedures, a high level of uncertainty often applies to the final results and their associated implications (Ooyama 1987; Mace and Ackerman 1996; Zhang et al. 2001a).

Recently, a variational form of objective analysis (VOA) was developed by Zhang and Lin (1997). This approach utilizes column-integrated conservation equations for mass, energy, momentum and moisture as well as top-of-the-atmosphere (TOA) and surface fluxes of energy, momentum, and moisture to constrain, via variational methods, the objective analysis. Application to actual ARM field program data shows that the VOA significantly reduces the sensitivity of the resulting diagnosed quantities, such as vertical velocity and advective tendencies, to factors such as the amount and types of data input into the analysis, the form of the interpolation procedures used for missing data, etc. (Zhang et al. 2001a, hereafter ZET). These encouraging results, along with the underlying principle behind the VOA, have led to the official adoption of the VOA by the ARM program (Zhang et al. 2001b). The promising nature of the VOA approach, including its expected extensibility in terms of utilizing additional constraints and forms of data, warrant continued development and validation efforts. For example, the inherent fact that the diagnosed quantities cannot be validated against the field observations themselves raises some questions regarding the accuracy of the VOA results, the validity of some of the less constrained aspects of its application and the actual level of improvement that is provided by the VOA over more conventional approaches.

To address the above questions, this paper presents an exploration of the efficacy of the VOA approach through the use of high-resolution numerical model simulation data. In short, we utilize the Naval Research Laboratory's Coupled Ocean/Atmosphere Mesoscale Prediction System (COAMPS; Hodur 1997) to provide cloud-resolving model simulation data of atmospheric variability, sample the output in a manner consistent with a typical field program, apply the VOA, and then compare the resulting VOA diagnosed quantities to the ''true'' domain-averaged values supplied by the model. This procedure provides a general test of the VOA performance including its dependence on a number of parameters and assumptions associated with its application. Moreover, it allows a way to test the sensitivity of the results to sampling timescales and space scales, sources of input data, synoptic condition, etc. In this way, it can be used to explore the benefits and limits that might be afforded to a particular field program by various observing system strategies. For example, given the resource intensive nature of atmospheric field programs, it would be beneficial to have additional insight into the relative scientific versus economic benefits of various sounding frequency or spacing approaches.

In the next section, the VOA is described. Section 3 describes the atmospheric model and the observational simulation procedure. Section 4 describes the methodology employed to assess the VOA, including the manner in which the VOA is applied to the model data. Section 5 presents the results of the comparisons between the analyzed sampled model data and the actual domain-averaged model quantities. Section 6 provides a summary of the results and discusses the implications of the results to ongoing and future atmospheric field programs.

2. Variational objective analysis

In practice, the VOA is typically applied to an initial estimate from observational data that has been through a preliminary form of analysis. This preliminary analysis typically includes steps to fill in missing data and possibly interpolate the data to a specified set of predetermined analysis points that are more conducive for computing derivatives and/or line integrals than the actual sites associated with the observational network. In addition to these data processing sorts of steps, the preliminary analysis may include other forms of processing such as application of smoothing, application of mass constraints, etc. The relative benefits of various ap-

proaches for performing this initial analysis are discussed in ZET and Zhang et al. (2001b). On top of this initial analysis, the VOA is applied to constrain the sounding data to be consistent with surface and TOA quantities. This is achieved by making minimum possible adjustments to the initial sounding analysis so that the final analysis yields column-integrated budgets of atmospheric mass, energy, water vapor, and momentum that are consistent with surface and TOA measurements. Therefore, whatever comes horizontally into the atmospheric column equals whatever comes out from the bottom and the TOA plus the increase of local storage of mass, energy, water vapor, and momentum. As discussed in ZET, there is an inherent limit in the accuracy of the initial sounding analysis. Adjustment of this initial analysis is justified as long as its magnitudes are within the expected error bounds.

For completeness, we briefly review the VOA scheme. Full details of the method and its application are described in Zhang and Lin (1997) and ZET. When the VOA is applied in the present context, the (model) sounding data are required to satisfy the following vertically integrated constraints:

$$\langle \nabla \cdot \mathbf{V} \rangle = -\frac{1}{g p_S} \frac{dp_S}{dt}, \tag{1}$$

$$\frac{\partial \langle q \rangle}{\partial t} + \langle \nabla \cdot \mathbf{V} q \rangle = E_S - \text{prec} - \frac{\partial \langle q_H \rangle}{\partial t}, \tag{2}$$

$$\frac{\partial \langle s \rangle}{\partial t} + \langle \nabla \cdot \mathbf{V} S \rangle = R_{\text{TOA}} - R_{\text{SRF}} + \text{SH} + L\text{prec} + L\frac{\partial \langle q_H \rangle}{\partial t}, \quad \text{and} \tag{3}$$

$$\frac{\partial \langle \mathbf{V} \rangle}{\partial t} + \langle \nabla \cdot \mathbf{V}\mathbf{V} \rangle - f\mathbf{k} \times \langle \mathbf{V} \rangle - \nabla \langle \phi \rangle = \boldsymbol{\tau}_s, \tag{4}$$

where the bracket represents vertical integration, $\mathbf{V}$ is the wind (with u and v components), q is the water vapor mixing ratio, $s = CpT + gz$ is the dry static energy, and p_s is the surface pressure. The net downward radiative flux at the TOA and at the surface (SRF) is R; $\boldsymbol{\tau}_s$ is the surface wind stress, prec is the precipitation, SH is the sensible heat flux, E_s is the surface evaporation, and q_H is the cloud hydrometeor mixing ratio. In the present study, terms on the left-hand sides of (1)–(4) are obtained from model output sampled at model ''sounding'' locations, and right-hand sides of (1)–(4) are derived from area-averaged surface and TOA model output. It is worth noting that the constraint on moisture is applied, both for this study and for observed analyses, on the column integral of moisture flux convergence $[\nabla_H \cdot (\mathbf{V}_q)]$ using a line integral estimate of the flux through the domain boundaries. Following the analysis, the advective $(\mathbf{V} \cdot \nabla_H q)$ and divergent $(q\nabla_H \cdot \mathbf{V})$ components of the moisture flux convergence are computed from the VOA adjusted values of wind and moisture. The dependence of the results on the inclusion of the hydrometeor term, the sampling associated with the area-averaged surface and TOA terms, as well as the lack of actual measurement error associated with the model will be addressed in the following sections.

The VOA adjustments to the soundings are determined by minimizing the following (scalar) cost function subject to the constraints associated with Eqs. (1)–(4):

$$\begin{aligned} I(t) = {} & (\mathbf{u}^* - \mathbf{u}_o)^{\mathrm{T}} \mathbf{Q}_\mathbf{u} (\mathbf{u}^* - \mathbf{u}_o) \\ & + (\mathbf{v}^* - \mathbf{v}_o)^{\mathrm{T}} \mathbf{Q}_\mathbf{v} (\mathbf{v}^* - \mathbf{v}_o) \\ & + (\mathbf{s}^* - \mathbf{s}_o)^{\mathrm{T}} \mathbf{Q}_\mathbf{s} (\mathbf{s}^* - \mathbf{s}_o) \\ & + (\mathbf{q}^* - \mathbf{q}_o)^{\mathrm{T}} \mathbf{Q}_\mathbf{q} (\mathbf{q}^* - \mathbf{q}_o), \end{aligned} \tag{5}$$

where subscript o in (5) denotes analysis from the initial interpolation schemes; superscript * denotes final analysis; the $\mathbf{Q}_\mathbf{s}$ are matrices that prescribe the weighting functions; and the variables $\mathbf{u}$, $\mathbf{v}$, $\mathbf{s}$, and $\mathbf{q}$ represent vectors (i.e., profiles). This procedure requires the specification of error estimates to determine the weights in the cost function (5). Note that it is the relative magnitudes of these estimates, rather than their absolute magnitudes that enter into the minimization procedure. Zhang and Lin (1997) specified these weights primarily from instrument and measurement uncertainty estimates. ZET modified this to include a component that is related to the observed standard deviations (versus pressure) of the atmospheric sounding data. This study follows the approach used in ZET except that the standard deviations are computed from the model output. These standard deviations are multiplied by 0.2 to provide an estimate of the aliasing errors; these values are then added to the instrument and measurement uncertainties used in Zhang and Lin (1997). Sensitivity tests of the analysis to the choice of error estimates is given in ZET with the result that uncertainties associated with the representation and sampling of the terms on the right-hand sides of (1)–(4) are larger than those associated with the specification of the range of error estimates considered in Zhang and Lin (1997) and ZET.

An example application of the VOA method to observed data from the summer 1995 ARM Southern Great Plans (SGP) IOP is presented in Fig. 1, with Fig. 2 illustrating the rainfall that was observed during this same period. The left panels of this figure show the vertical velocity diagnosed from an initial sounding analysis using a number of different input data choices and/or reasonably posed analysis schemes. Evident is the drastic variation in the results from these initial analyses. It is important to keep in mind that these are typically the ''final'' results of a given analysis for a field program and thus the differences exhibited between the results in the left panels illustrates the type of uncertainty associated with the final results. The right panels of Fig. 1 show the results after the VOA has been applied to the initial analyses. While there is still some

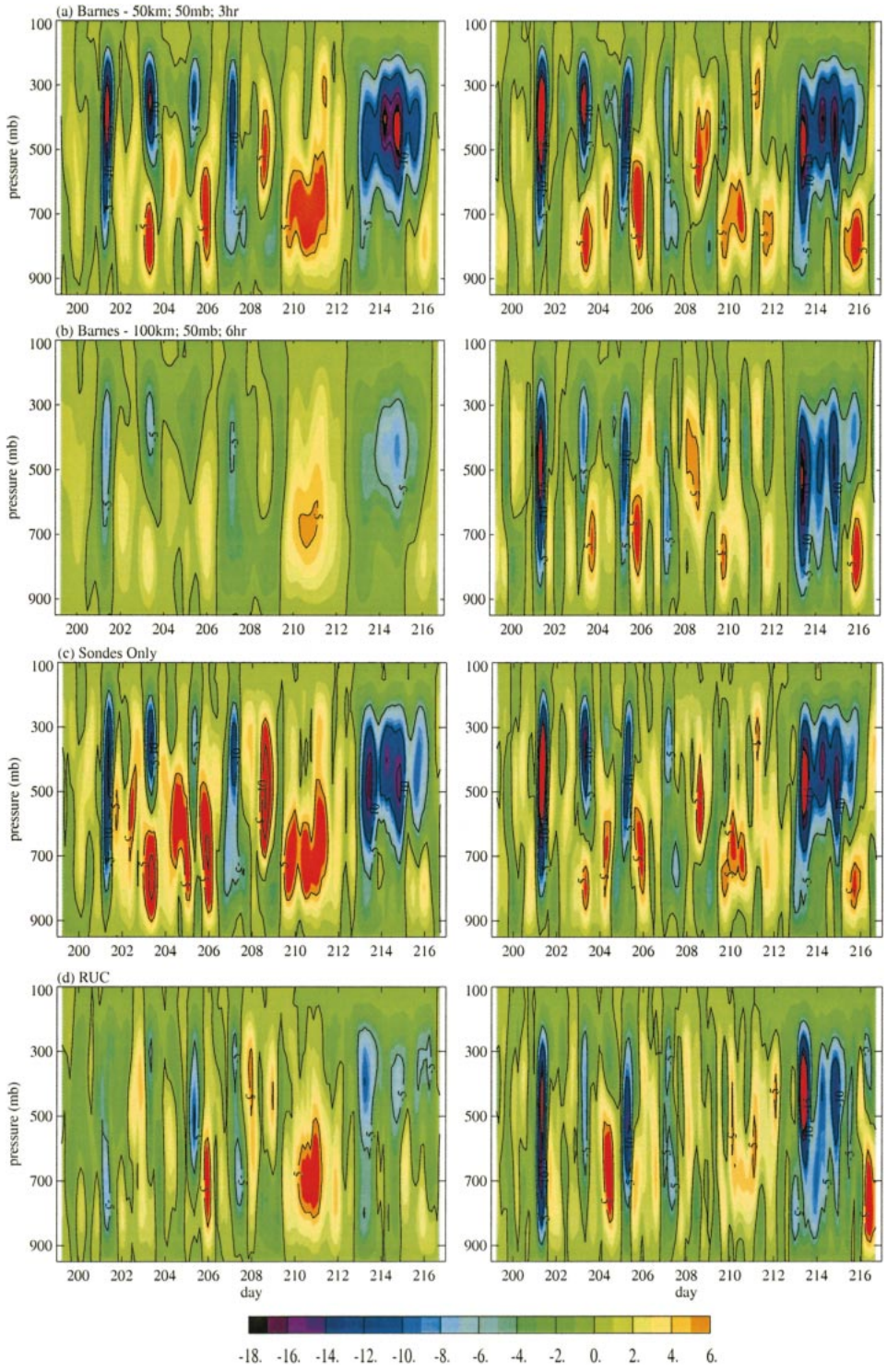

FIG. 1. Sensitivity of the analysis of the pressure vertical velocity omega (hPa h^{-1}) to various implementations of the VOA scheme. (left) (a) Analyzed pressure vertical velocity (hPa h^{-1}) using one iteration of the Barnes interpolation scheme with a mass balance constraint and length scales of (L_x, L_y, L_p, L_t) = (50 km, 50 km, 50 hPa, 3 h) using both radiosondes and wind profiler data. (b) Same as (a), except for (L_x, L_y, L_p, L_t) = (100 km, 100 km, 50 hPa, 6 h). (c) Same as (a), except for the Cressman scheme (L_x, L_y, L_p, L_t) = (50 km, 50 km, 50 hPa, 6 h), three iterations using radiosondes only. (d) Same as (c), except using the NOAA Rapid Update Cycle analyses instead of the radiosondes. (right) Same as corresponding left panel, except after applying the VOA. More details can be found in ZET.

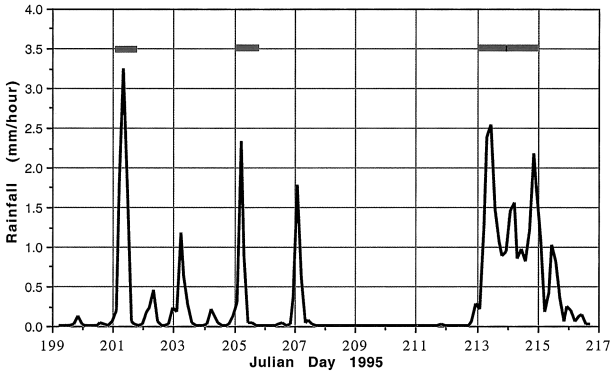

FIG. 2. Analyzed precipitation for the Jul 1995 ARM SGP IOP. Day 200 corresponds to 19 Jul 1995. COAMPS simulations were performed for the four 24-h periods indicated by the thick horizontal bars.

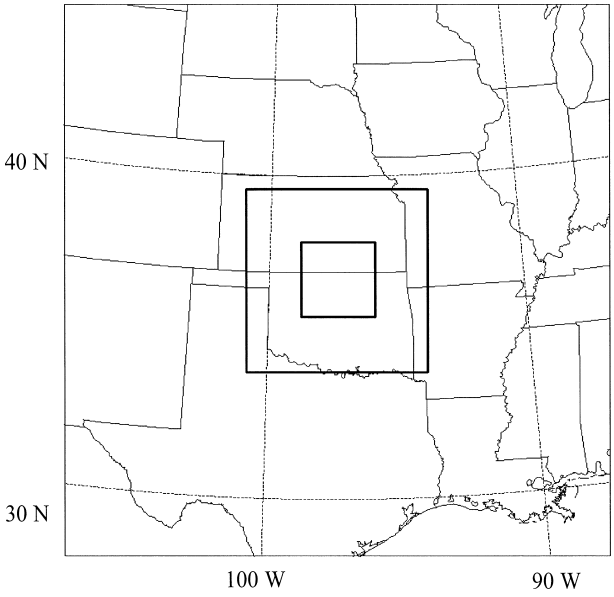

FIG. 3. COAMPS grid configuration. The outer domain is represented by a 70 × 70 gridpoint mesh with 27-km resolution. The intermediate domain is represented by a 70 × 70 gridpoint mesh with 9-km resolution. The inner domain, centered at 36.6°N and 97.5°W, is represented by an 85 × 85 gridpoint mesh with 3-km resolution.

variation between the final vertical velocity profiles, the results are considerably more consistent than without the application of the VOA. This feature, along with knowing that it has come about by balancing the vertically integrated budget equations with observed flux quantities, provides considerably more confidence in the VOA results. Of course the question still remains, how close are the VOA estimates of vertical velocity, as well as other estimated quantities (e.g., advection terms), to the true values. Assuming there are nontrivial differences between the VOA estimates and the observed values, it would be useful to know how big the remaining errors are relative to the observed variability and how they depend on factors such as synoptic conditions, input data sources, sampling timescales and space scales. As indicated above, this article utilizes a high-resolution model to provide a synthetic yet realistic atmosphere that can be sampled along the lines of a field program in order to explore some of the above questions.

3. COAMPS ARM simulation data

a. Model and simulation procedure

The COAMPS simulation data for the present study are taken from a series of forecasts for the summer 1995 ARM SGP IOP. The ARM simulations are carried out using a triple-nested version of COAMPS with horizontal grid dimensions of 27, 9, and 3 km. A total of 30 vertical levels are used, with highest resolution near the surface. The COAMPS analysis and initialization were run utilizing a 12-h update cycle, and at least 48 h of spinup time was allowed prior to the start of each of the forecasts chosen for the present variational analysis tests. Lateral boundary data from the Navy Operational Global Atmospheric Prediction System (NOGAPS; Hogan and Rosmond 1991) were employed using Davies (1976) boundary conditions. No feedback was allowed from the inner nests to the parent nests. Subgrid-scale mixing is computed using the scheme of Mellor and Yamada (1974), and surface fluxes are computed using the treatment of Louis et al. (1982). For the outer mesh, the convective parameterization of Kain and Fritsch (1990) is used, but convection is modeled explicitly in the inner meshes. In the research version of COAMPS employed here, the microphysics scheme of Ferrier (1988) is used rather than the Rutledge and Hobbs (1983) scheme, which is standardly used in COAMPS. The Ferrier scheme includes a bulk parameterization of the graupel/hail phase, which can be important for simulations of convection on the Great Plains. Radiation is treated following Harshvardhan et al. (1987), and clouds are parameterized using the diagnostic cloud parameterization of Slingo (1987).

A plot of the COAMPS grid configuration used for the simulations is shown in Fig. 3. The present work focuses on the quasi-cloud resolving 3-km inner-mesh grid, which was centered at 36.6°N and 97.5°W. This position is near the central site of the ARM SGP Cloud and Radiation Testbed (CART), a roughly square region with sides approximately 350 km in length in north-central Oklahoma and south-central Kansas. The 3-km mesh grid has 85 × 85 grid points in the horizontal, so the horizontal dimensions of the domain are approximately 2/3 the dimensions of the CART. For this work, 4 days from the summer 1995 SGP IOP were selected based on the presence of significant precipitation events. Tests suggest that the VOA has an appreciable impact in such cases. The days selected are 20 July, 24 July, 1 August, and 2 August (see Fig. 2). A description of the synoptic conditions during the IOP is provided in

ZET. For each of these days, a 24-h forecast was carried out.

b. Data for VOA experiments

The COAMPS forecast data are assumed here to provide a representation of the atmosphere that is adequate in its realism for the present VOA assessment. Although the simulations were successful insofar as producing rainfall on the selected days, the validity of the present methodology is not particularly dependent on forecast accuracy, which depends on issues such as initial conditions. More pertinent is the fact that the general characteristics of the present simulations appear realistic, including the large-scale correlation between midlevel vertical motion and precipitation, which was compared with ARM data (not shown). Although the 3-km dimension of the COAMPS inner mesh used here is rather coarse for a cloud-resolving study, its use has some support from previous studies. For example, Weisman et al. (1997) found that a 4-km horizontal grid dimension was adequate to represent convective momentum and heat transports in midlatitude squall-line-type convection. In addition, Petch and Dudhia (1998) reported success in explicit simulations of ARM convection in June 1993 using a 6.67-km horizontal grid mesh.

For each of the forecasts, data necessary for running and validating the VOA, including soundings and area-mean flux data, were saved once every 12 min during the simulations for selected domains. The flux data that were saved are the time-mean values between the sounding times. Relevant quantities of interest for validation, including the vertical velocity ω and advective tendencies of temperature and moisture, were also saved. The domains and sounding sites for which data were saved are shown in the upper panel of Fig. 4. The box comprising the entire region is 216 km on a side, and corresponds to a 72 $\times$ 72 subdomain of the entire 85 $\times$ 85 3-km inner-mesh grid (see Fig. 3). In addition there are 4 boxes of side 108 km, and 16 boxes of side 54 km that occupy the same area as the 216-km box. In total then, there are 21 sounding arrays (i.e., boxes) occupying the area shown in the upper panel Fig. 4 (1 large, 4 intermediate, and 16 small arrays). For each of these boxes, data are saved from a (model derived) sounding network of Nine sites, as illustrated by Fig. 4. The lower panel of Fig. 4 schematically depicts the sorts of questions being considered in this study with regard to the VOA, and which can be examined using the model data sampling described above. For example, what is the impact of using five versus nine sounding sites in the VOA? What are the impacts on the apparent accuracy of the VOA to the spatial and temporal sampling characteristics of the data (e.g., 3-versus 6-h sampling or 100 km versus 200 km domains)?

As mentioned in the introduction, diagnostic quantities such as horizontal and advective tendencies are particularly sensitive to the type of objective analysis scheme applied and yet the derivation of these quantities is usually of significant relevance to reaching the desired goals of a given field experiment. In this study, the vertical velocity and the advective tendencies are the principal benchmarks used to examine the performance of the VOA. In order to validate the advective tendency estimates made by the VOA, the horizontal and vertical advective tendencies are saved from the COAMPS simulations corresponding to each of the 21 boxes in Fig. 4. For this purpose, horizontal advective tendencies of potential temperature and moisture variable mixing ratios from COAMPS are simply averaged across the boxes. Using subscript H to denote large-scale horizontal advective tendencies, one obtains

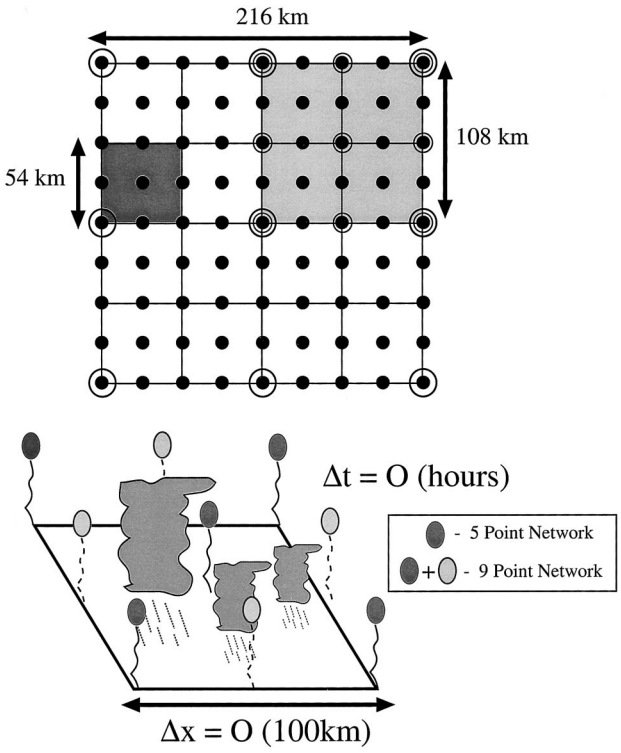

FIG. 4. (upper) Schematic representation of the spatial sampling of soundings (black dots) from the model's 3-km mesh grid (see Fig. 3). Three horizontal sampling scales are represented. The largest scale is represented by one 216 km $\times$ 216 km subdomain (white box), with sounding locations represented by the nine large circles. The intermediate scale is represented by four 108 km $\times$ 108 km subdomains. The light gray box is an example of one of these regions, with its sounding locations represented by the 9 small circles. The smallest scale is represented by sixteen 54 km $\times$ 54 km subdomains. The dark gray box is an example of one of these regions, with nine black dots representing the corresponding sounding sites. In total, there are 21 sounding arrays (i.e., boxes) occupying the area shown (1 large, 4 intermediate and 16 small arrays). (lower) Idealized depiction of a given atmospheric model sounding array using five profiles (one at the center and four at the corners) and nine profiles. The array covers a region that has dimensions on the order of 100 km and the sampling frequency is on the order of hours.

$$\left(\frac{\partial q}{\partial t}\right)_H = \overline{\left(-u\frac{\partial q}{\partial x} - v\frac{\partial q}{\partial y}\right)}, \quad (6)$$

where q denotes mixing ratio or potential temperature, u and v represent the horizontal wind components, and the overbar denotes averaging over a selected domain. The large-scale vertical advective tendencies are computed similarly, but in this case a quantity representing the contribution of small-scale (in this case the 3-km mesh grid scale) vertical motions is subtracted from the area-mean tendencies. Using subscript V to denote large-scale vertical advective tendencies, one obtains

$$\left(\frac{\partial q}{\partial t}\right)_V = \overline{-w\frac{\partial q}{\partial z}} - \overline{\left(-\frac{1}{\rho}\frac{\partial(\rho q' w')}{\partial z}\right)}, \quad (7)$$

where w is vertical velocity, ρ is density, and primes denote deviations from the area-mean. The vertical velocity and advective tendencies were first computed on the COAMPS terrain-following coordinate, and then interpolated to 40 constant pressure surfaces.

4. VOA experiment methodology

As described above, the model data employed for examining the VOA consists of four 24-h simulations (Fig. 2). Model output is sampled in a manner consistent with an atmospheric field program using three different size domains (54, 108, and 216 km; see Fig. 4). Profiles of temperature, horizontal velocity, water vapor, and hydrometeor quantities are saved every 12 min at specific sounding locations (Fig. 4). Domain-averaged sounding data are also saved every 12 min, along with domain-averaged vertical velocity and surface pressure. Domain- and time-averaged surface and TOA fluxes and advective tendency data are computed for the intervening 12-min periods. The surface pressure and flux data are used as constraints on the VOA. The vertical velocity and advective tendencies are used for validation purposes, that is, the true values against which the VOA estimates are compared.

The base case analysis consists of evaluating the VOA when applied to model sounding data with a temporal sampling of 3 h and a spatial sampling of 108 km (e.g., the light gray box in Fig. 4). In this case, instantaneous model soundings, sampled every 3 h, are used in Eqs. (1)–(5) in conjunction with domain-averaged and (3 h) time-averaged flux and surface pressure tendency data (hereafter, forcing data). Specifically, profiles of u, v, T, and q are used in the left sides of Eqs. (1)–(4) as well as in Eq. (5) to derive the adjusted profiles (e.g., u^*). The area- and time-averaged forcing data consist of surface pressure and pressure tendency in Eq. (1); surface precipitation and evaporation in Eq. (2); surface precipitation, sensible heat flux, and surface and TOA net radiation in Eq. (3); and surface wind stress in Eq. (4). Note that for the base case, the forcing term based on the storage of hydrometeors (e.g., liquid, rain, hail) is set to zero. This specification is consistent with the VOA's application to observed data since these terms are typically very difficult to obtain from observations; an exception is the use of microwave-derived cloud liquid water for ARM. As discussed in section 2, the weighting terms in Eq. (5) are derived using the same procedures as in ZET, with the standard deviations versus pressure computed from the 12-min data from all nine sounding locations and all 21 subdomains (see Fig. 4) over the given 24-h period being analyzed. Note that the above methodology assumes error-free estimates of surface and TOA fluxes as well as no instrument errors associated with the sounding data. The dependence of the results on this assumption will be tested in section 5d via additional sensitivity experiments that use artificially supplied error characteristics for the input data.

In order to determine the level of improvement of the VOA over more conventional analyses, a reference analysis is also computed from the model soundings that only utilizes the mass constraint associated with the VOA [i.e., Eq. (1)] since applying some form of mass constraint is a fairly common practice (O'Brien 1970; Lin and Johnson 1996). Thus, the reference analysis consists of pseudo-domain-averaged values (using a simple five-sounding average) for temperature and moisture, with winds, and therefore vertical velocity and advection terms, that have been adjusted via the mass constraint only. Note that since there is no missing data associated with the model soundings, there is no need for the type of gap-filling procedures discussed at the beginning of section 2. By comparing the analyzed quantities (e.g., vertical velocity and advection terms) derived from the complete VOA analysis as well as from the reference analysis to the model's true time- and domain-averaged values, the additional improvement that the VOA might provide over more conventional analysis approaches can be examined. It is worth emphasizing that since the reference analyses uses the same preprocessing procedure as the VOA, their differences are expected to be smaller than would be the case for two analysis schemes that included differences in the initial preprocessing steps as well.

Following from the base case analysis described above are a number of sensitivity tests to determine the impact of 1) using additional soundings (e.g., nine instead of five; see Fig. 4), 2) altering the sampling frequency (e.g., 1 or 6 h instead of 3 h), 3) altering the array size (e.g., 216 or 64 km, instead of 108 km), 4) employing the known hydrometeor forcing term in Eqs. (2) and (3), and 5) adding noise to the model soundings in order to incorporate the effects of instrument error into the sampling.

5. Results

a. Base case

Figure 5 illustrates a comparison of the analyzed vertical velocity from the soundings and their associated

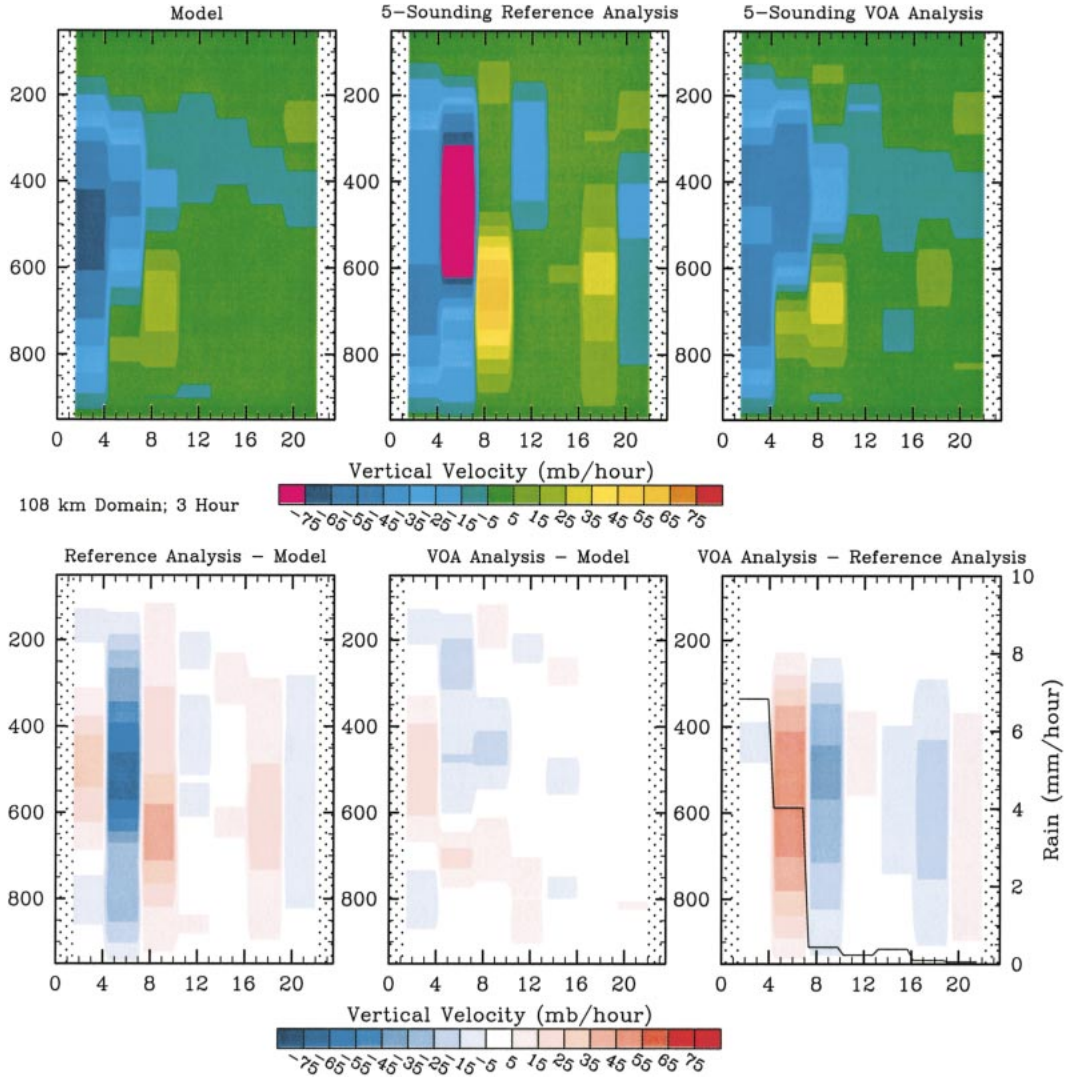

FIG. 5. Analysis and model intercomparison results for 1 Aug 1995 in terms of diagnosed vertical velocity, 3-h sampling and a 108-km domain (see discussion of base case in section 4). (upper-left) The model time- and domain-averaged vertical velocity values for the northwest intermediate size domain (i.e., upper-left 108-km box in Fig. 4). [upper-middle (right)] The analyzed vertical velocity values using the VOA with mass-only (all) constraints. [lower-left (middle)] The difference between the analyzed vertical velocity values using the VOA analysis with mass-only (all) constraints and the model time- and domain-averaged values. (lower-right) The difference between the analyzed vertical velocity values derived using the VOA with all constraints and using the mass-only constraint. Line plot shows the domain-averaged precipitation for this domain.

errors relative to the model's true domain-averaged values based on the 1 August 1995 simulation using the five-sounding network from the upper-left 108-km grid (see Fig. 4) and 3-h sampling. The three panels in the upper row show the vertical velocity from the model, reference analysis and VOA analysis, respectively. The three panels in the lower row show the difference in vertical velocity between the reference analysis and model values, the VOA analysis and the model values, and the VOA and reference analysis values, respectively. The line plot in the lower-right panel indicates the domain-averaged rainfall for this domain. Examination of these panels shows that while both the reference and VOA analysis capture the bulk characteristics of the variability (e.g., significant upward motion during the rain event), the VOA values exhibit considerably smaller errors (about half the size) compared to the values from the reference analysis. Closer inspection shows that errors associated with the reference values have a magnitude similar to the size of the vertical velocity field itself. This is in fact the case, during both disturbed and undisturbed periods. At this stage it is worth emphasizing that because the vertical velocity and related fields (e.g., vertical advection) have significant temporal and spatial variability, direct differencing is a rather stringent test since small errors in the timing or place-

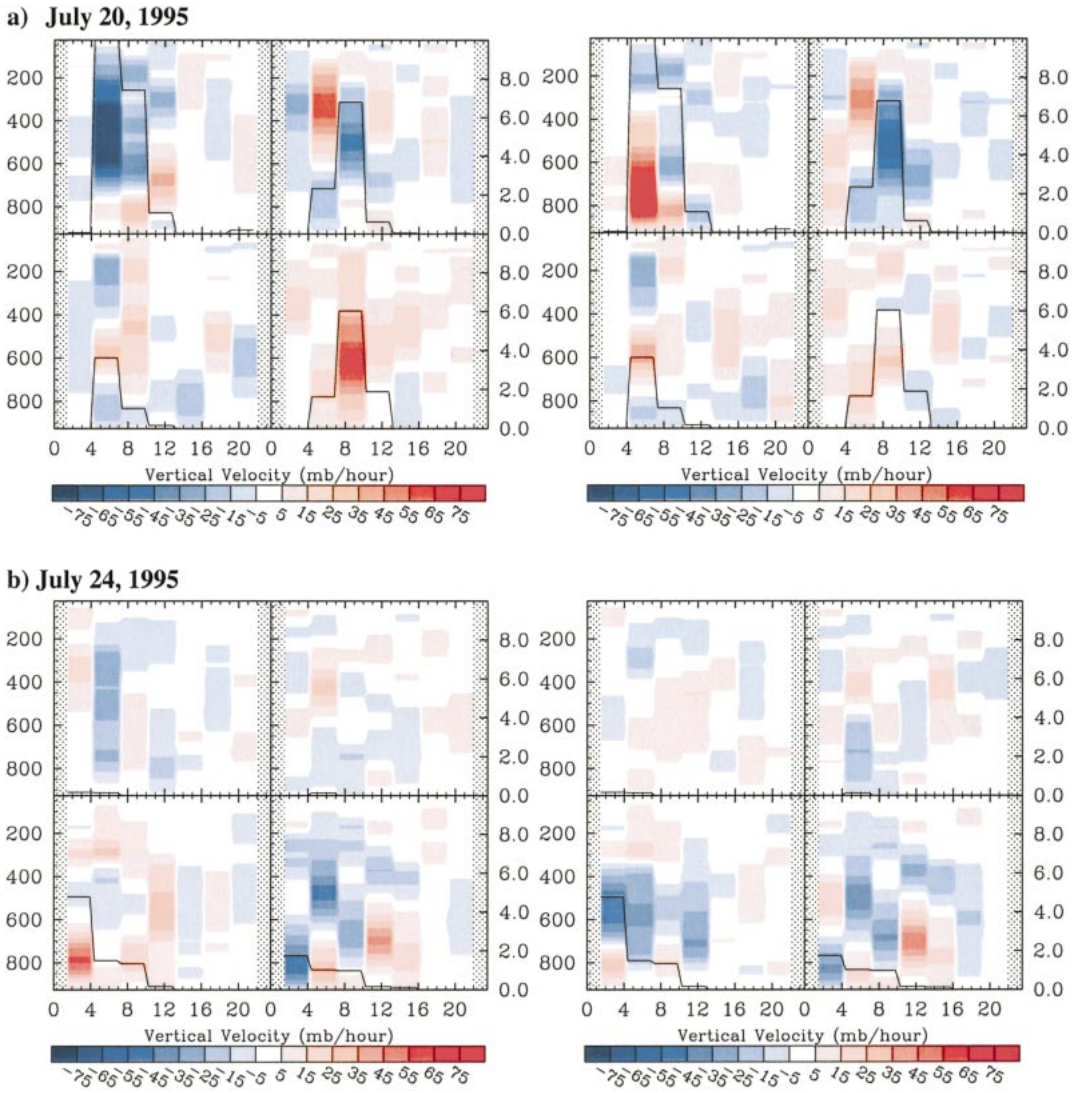

FIG. 6. Analysis and model intercomparison results for (a) 20 Jul 1995, (b) 24 Jul 1995, (c) 1 Aug 1995, and (d) 2 Aug 1995 in terms of diagnosed vertical velocity, 3-h sampling, and all four 108-km domains (see discussion of base case in section 4). [left (right)] The difference between the analyzed vertical velocity values using the VOA with mass-only (all) constraints on the model soundings and the model time- and domain-averaged values. The upper-left plot of each panel corresponds to the northwest domain of the four 108-km domains; the upper-right plot corresponds to the northeast domain, etc. The labels on the left vertical axis are in hPa. The labels on the bottom horizontal axis are in hours. The labels on the right vertical axis are in mm h^{-1} and provide the scale for the line plot in each panel, which represents model domain-averaged rainfall.

ment of convection could result in significant errors in the diagnosed quantities. In any case, the main message, at least for this case, is that the VOA analysis is in considerably better agreement with the model time- and domain-averaged values than the reference analysis.

The comparison discussed above indicates a fairly significant improvement in the analyzed vertical velocity values associated with VOA analysis over the reference analysis. To examine how dependent this improvement might be on the synoptic condition, Fig. 6 illustrates similar comparisons for all four of the 108-km domains for all four model forecast days. Each four-panel composite plot shows the analysis error for the four 108-km domains for a given forecast day. Each panel within the four-panel composite is analogous to the lower-left or lower-center panels of Fig. 5. The four-panel composite plots on the left (right) are for the reference (VOA) analysis. In each case the line plots within the panels show the domain-averaged rainfall for the given domain for the given forecast day. Comparing the errors for 20 July 1995 (Fig. 6a) shows for the most part rather modest improvements by the VOA over the reference analysis over the course of the 24-h period. For example, for the upper-left domain the significant negative error that occurs over most of the atmospheric column during the second 3-h period in the reference

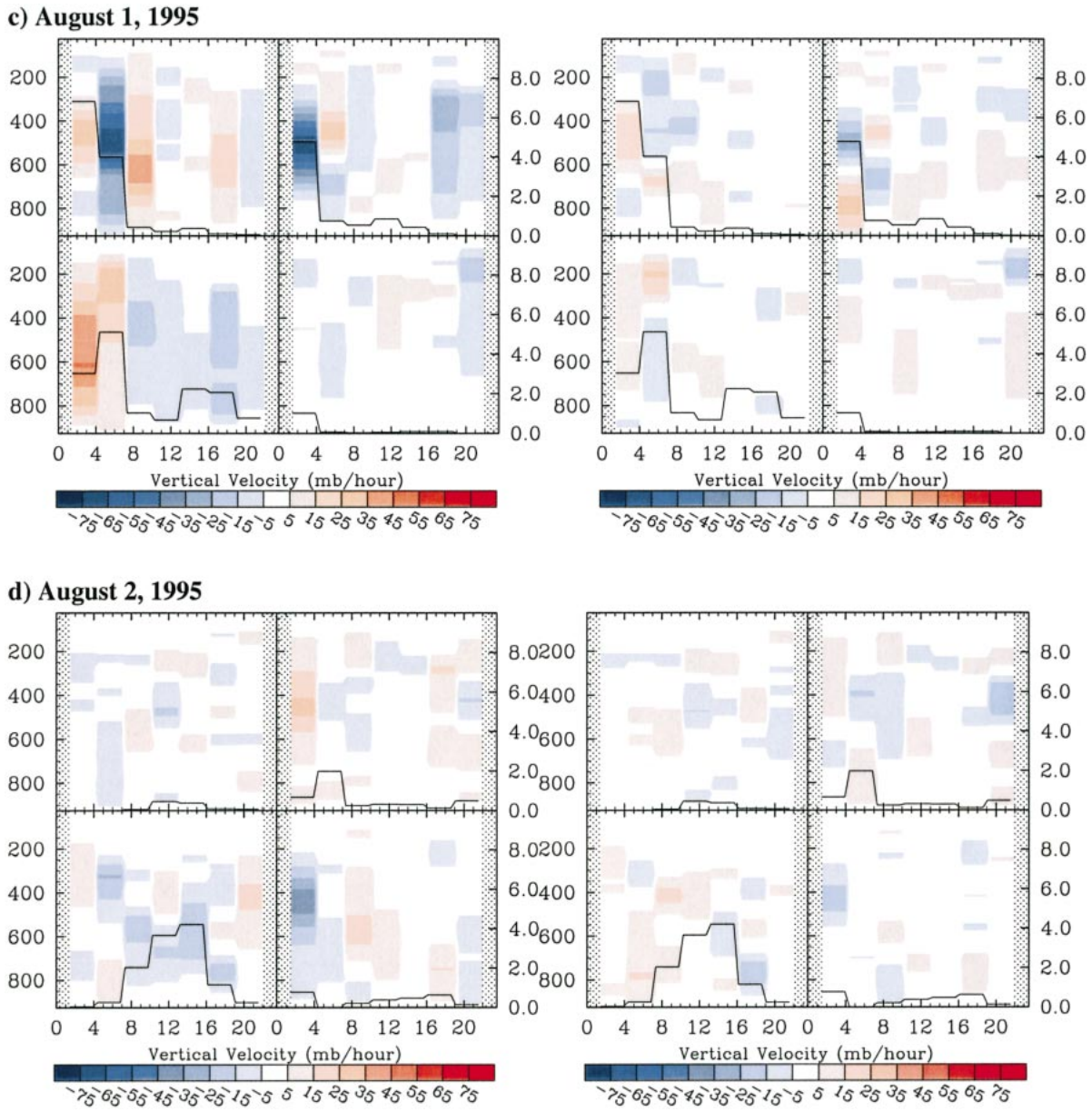

FIG. 6. (*Continued*)

analysis changes structure somewhat in the VOA but more importantly does undergo a bit of a decrease in magnitude. Out of the following four 3-h periods in this domain, there is a modest decrease in the error associated with the VOA over the reference analysis for the first and last of these periods, while for the other two 3-h periods there is no noticeable improvement. Similar levels of improvement occur for the other three domains for this forecast day, with the most noticeable improvement occurring in the lower-right domain during the peak precipitation event at about forecast hour 8.

Comparing errors for the 24 July 1995 simulation shows some improvement by the VOA for the biggest errors in the upper-left domain, very little improvement for the upper-right and lower-right domains and to some extent a modest increase in the error for the lower-left domain. It should be noted that overall the precipitation and the magnitude of the vertical velocity variations of the 24 July 1995 simulation are considerably smaller than for the 20 July 1995 case. This is in fact consistent with the observed precipitation record shown in Fig. 2. Comparing errors for 1 August 1995 shows evidence of the greatest improvements associated with the VOA over the reference analyses. In all but the lower-right domain, which has very little precipitation, the VOA errors are significantly less than those associated with

the reference analysis. Finally, for the 2 August 1995 simulation, the errors are noticeably smaller for the VOA values compared to the reference analysis in all but the upper-left domain, for which there are comparable size errors under conditions that are fairly undisturbed. In summary, the comparisons above qualitatively indicate significant and somewhat uniform improvements in the diagnosed vertical velocity by the VOA as compared to the more traditional reference analysis. These improvements tend to be greatest during disturbed conditions, with errors typically being smaller and comparable between the two types of analysis during undisturbed conditions.

b. Sampling dependence

In order to examine the dependence of the error characteristics between the VOA and reference analyses on sampling conditions, the qualitative comparisons described in the previous section have been quantified in the middle panel of Fig. 7. This panel shows the root-mean-square (rms) vertical velocity errors for the VOA (red solid) and reference (green solid) analyses computed over all four forecast days, for all four 108-km domains (see Fig. 4) and for 3-h sampling. Also shown is the standard deviation of the model's time- and domain-averaged vertical velocity for the same sampling conditions (blue solid). Consistent with the qualitative discussion above is the fact that the VOA vertical velocity errors are typically smaller than the errors from the reference analyses. This reduction in error tends to be confined to the region between about 200 and 700 hPa, and amounts to as much as about 30% at around 500 hPa. An important consideration is the fact that over this same region of the troposphere, the VOA errors are about half the size of the variability itself while the reference errors are of nearly the same magnitude as the variability.

The other eight panels of Fig. 7, those surrounding the center panel, show the same information except for different sampling characteristics. The sampling characteristics for a given panel are described in the lower-right portion of each panel. Comparing panels vertically allows an examination of the dependence of the errors on spatial domain size (i.e., 54, 108, and 216 km) for a given temporal sampling. Comparing panels horizontally allows an examination of the dependence of the errors on temporal sampling (i.e., 1, 3, and 6 h) for a given domain size. A number of aspects are worth highlighting from the comparison of these panels. First, for the most part the errors from the VOA analyses are considerably less than errors from the reference analysis over most of the atmospheric column. Moreover, the errors from the VOA analysis are typically considerably less than the model variability, a feature that is less predominant for the reference analyses. Second, the errors for both types of analyses increase as the spatial domain decreases. Given that this reduction scales almost with the change in the domain size (i.e., factors of 2), this aspect of the error dependence is thought to arise simply from the errors in the derived gradients. For example, the size of a typical aliasing error associated with the wind values from the model's soundings is, at least at these scales, independent of the domain size, so that the size of the error of a horizontal gradient (i.e., divergence) is roughly inversely proportional to the domain size. Third, frequent temporal sampling on a large domain appears to be more favorable for either type of analysis. For example, errors for both analyses are least, and overall amount to a smaller fraction of the magnitude of the model variability for a sampling frequency of 1 h on a 216-km grid. On the other hand, the errors for both types of analysis exceed the model variability for a sampling frequency of 6 h on a 54-km domain.

In terms of practical considerations, the above results suggest that large array spacing is advantageous. Thus for the sampling conditions considered here, 216 km would be the domain size that leads to the smallest errors in vertical velocity. Based on this domain size, the 6-h sampling may be in fact the preferred sampling. This conclusion is based on two considerations. First, 6-h sampling is considerably more economical than 3- or 1-h sampling. Second, while the errors for the reference analyses increase with temporal sampling, the errors for the VOA analysis remain about the same size regardless of whether the sampling frequency is 1, 3, or 6 h. This independence of VOA error on sampling frequency, at least at this domain size, derives from the fact that time-averaged surface and TOA fluxes in the intervening periods are used to constrain the analyzed values, whereas this information is not taken advantage of by the reference analyses. However, it is worth noting that size of the error (red solid) relative to the variability itself (blue solid) tends to be smaller for the 1-h versus the 6-h sampling. This implies that more of the variability is accurately portrayed for the more frequent sampling, but this improvement is rather modest. In summary, for the sampling conditions considered here (i.e., $\sim$50–200 km), and apart from caveats associated with the approach and model's realism, the preferred sampling strategy is a relatively large spatial domain with a sampling frequency that can be as large as 6 h. This conclusion, however, is based on a comparison of absolute errors (i.e., Fig. 7) when comparing the different sampling strategies that may not necessarily be the appropriate metric, given that smaller domains will typically exhibit stronger variability. Moreover, it rests on the requirement that adequate surface and TOA fluxes are available to constrain the VOA. If such information is not available, then more frequent temporal sampling is preferred.

c. Advective quantities

Thus far, the comparisons have been solely based on vertical velocity. However, the vertical and horizontal

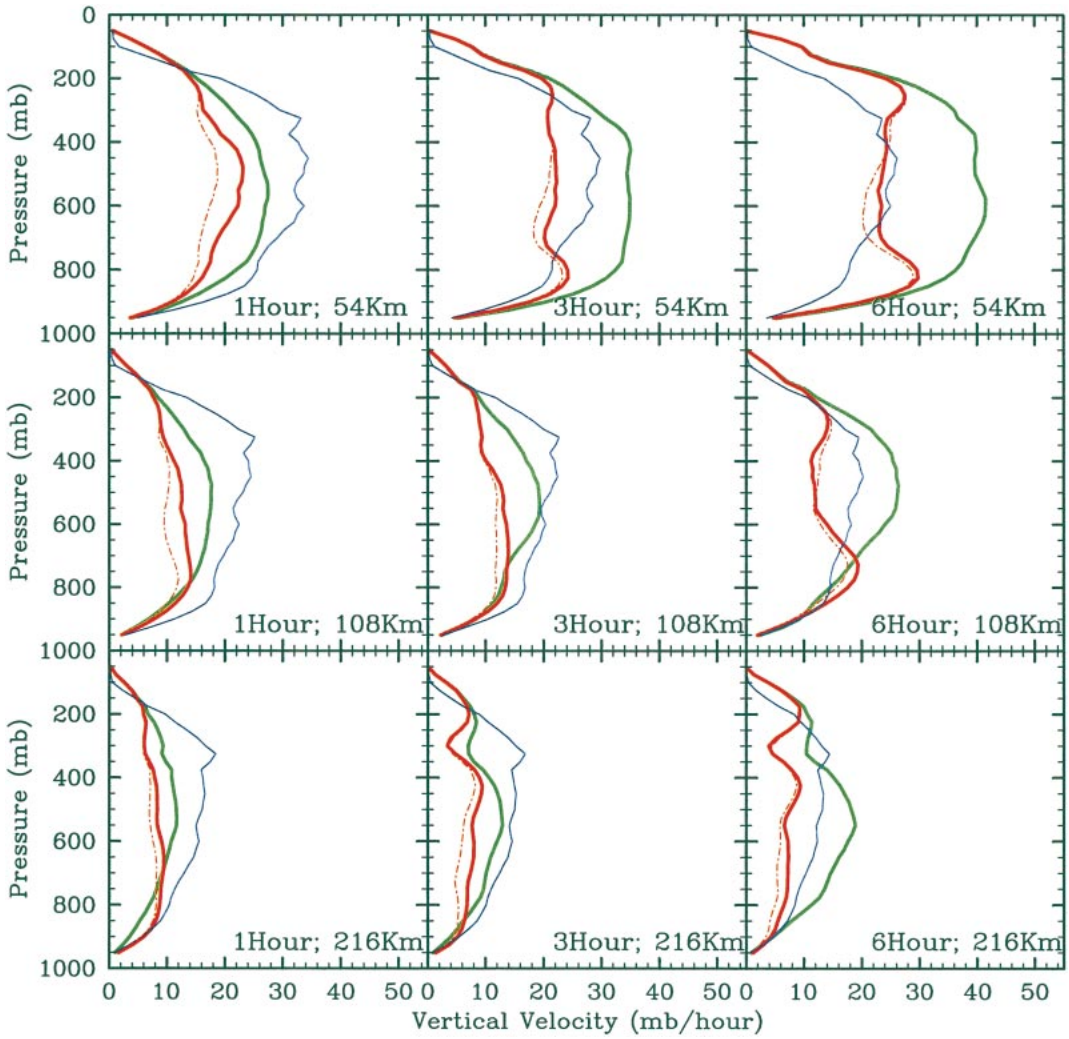

FIG. 7. Combined analysis and model intercomparison results for all simulation days: 20 Jul 1995, 24 Jul 1995, 1 Aug 1995, and 2 Aug 1995, in terms of diagnosed vertical velocity. Blue solid lines show std dev of model time- and area-averaged values. Red (green) solid lines show the rms differences between the VOA with all (mass only) constraints applied to the model soundings and the model's time- and domain-averaged values. Red dotted lines show the rms differences between the VOA with all constraints applied, including the use of the model's microphysics budget (see section 5), to the model soundings and the model's time- and domain-averaged values. The labels in the lower-right corner of each plot indicate the temporal and spatial samplings of the model soundings (see section 4).

advective and horizontal convergence terms are also important quantities diagnosed from an observational analysis. Given the improvements described above in analyzed vertical velocity by the VOA over the reference analyses, it is expected that such improvements would carry over to vertical advection of temperature and water vapor. Figure 8 shows the same information as Fig. 7, except for diagnosed vertical advection of temperature. Due to the fact that adjustments to temperature are inherently small ($\sim<0.2$ K), and thus in this case the changes to the vertical gradients are also relatively small, the characteristics associated with the errors in vertical advection of temperature closely mimic those associated with vertical velocity. This includes the comparison between VOA and reference analyses as well as their dependence on sampling conditions. The one exception to this is that the magnitudes of the errors are largest at around 200–250 hPa. The values of the model's vertical temperature gradient tend to be largest (not shown) near this level and thus a given size temperature error in this region is likely to have a larger effect on the vertical temperature advection.

Figure 9 shows the same information as Figs. 7 and 8, except for diagnosed vertical advection of moisture. Analogous with the vertical temperature advection errors, the errors for this quantity tend to peak in the lower atmosphere ($\sim$700–900 hPa) where the vertical gradient in moisture is largest. Apart from this difference, nearly all the previous conclusions drawn from the discussion of Fig. 7 regarding sampling issues and benefits of the VOA still apply when considering vertical advection of either temperature or moisture.

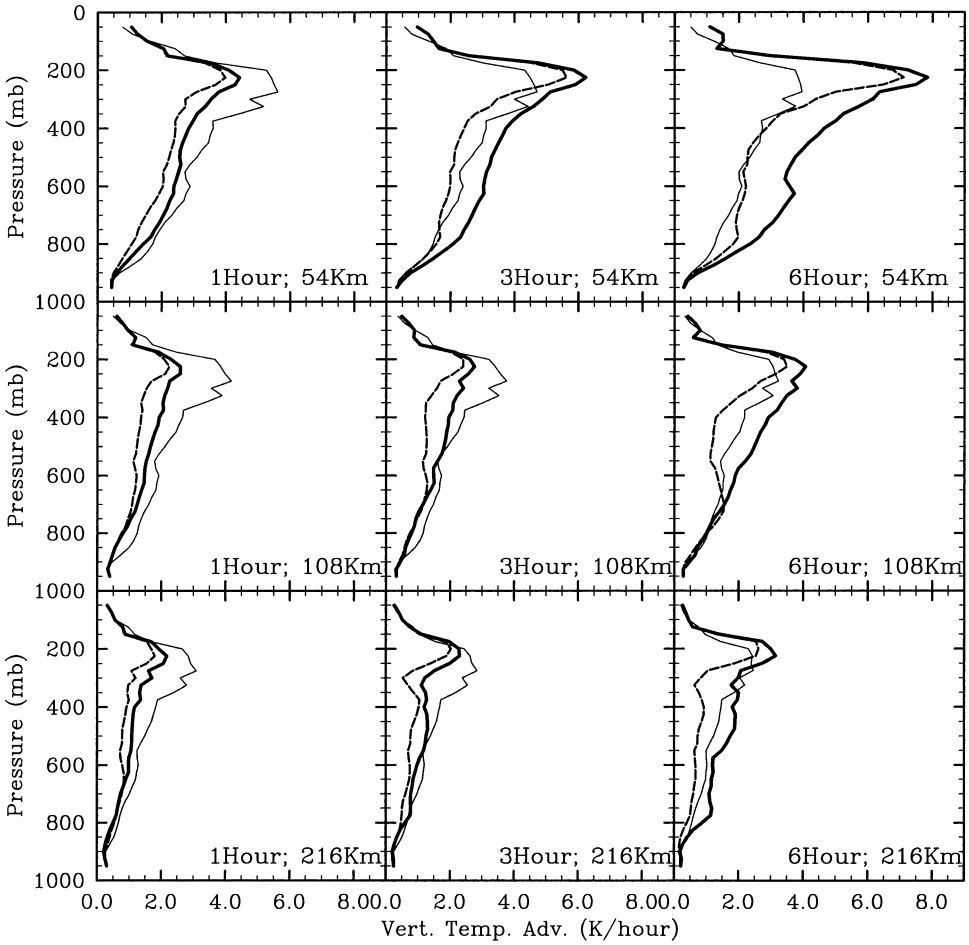

FIG. 8. Combined analysis and model intercomparison results for all simulation days: 20 Jul 1995, 24 Jul 1995, 1 Aug 1995, and 2 Aug 1995, in terms of diagnosed vertical advection of temperature. Thin solid lines show std dev of model time- and domain-averaged values. Dashed (solid) lines show the rms differences between the VOA with all (mass only) constraints applied to the model soundings and the model time- and domain-averaged values. The labels in the lower-right corner of each plot indicate the temporal and spatial samplings of the model soundings (see section 4).

Figure 10 illustrates the error characteristics for the horizontal moisture flux convergence $[\nabla_H \cdot (\mathbf{V}_q)]$, a quantity that is directly constrained by the VOA method and associated observations. As expected, the variability in this quantity is highest in the lower troposphere. Note that for the cases considered in this study, the variability (and associated errors) in the convergent component $(q\nabla_H \cdot \mathbf{V})$ of the moisture flux convergence is about four times that of the advective component $(\mathbf{V} \cdot \nabla_H q)$. In contrast to the vertical velocity and vertical advection terms, there is no obvious systematic level-by-level improvement associated with the application of the VOA for this quantity. In addition, the errors from both analysis procedures are the same order of magnitude as the model variability being diagnosed. This latter feature is also in contrast to the error characteristics for the vertical velocity and vertical advection terms where the typical errors in the diagnosed values were smaller than the model variability, at least for some sampling conditions (e.g., larger domain, higher frequency). The above two features hold true for the horizontal wind divergence and the horizontal advective tendencies as well. This is somewhat to be expected since the adjustments to horizontal wind, moisture and temperature are relatively small (i.e., within instrument error; see section 2). For example, in the case of horizontal moisture advection, the domain-averaged wind used in the calculation of the horizontal advection terms changes by very little, and given the relatively large size of the sampling domain, the horizontal gradients exhibit very minor adjustments via the VOA as well. In the end, horizontal advective/divergent quantities change very little upon application of the VOA and thus cannot exhibit a significant level of improvement compared to the truth—in this case the model.

The above result regarding the horizontal advective/divergent quantities warrants further discussion as it demonstrates an inherent limitation of the VOA method. To better illustrate this limitation, as well as the manner the VOA produces adjustments, Fig. 11 shows a com-

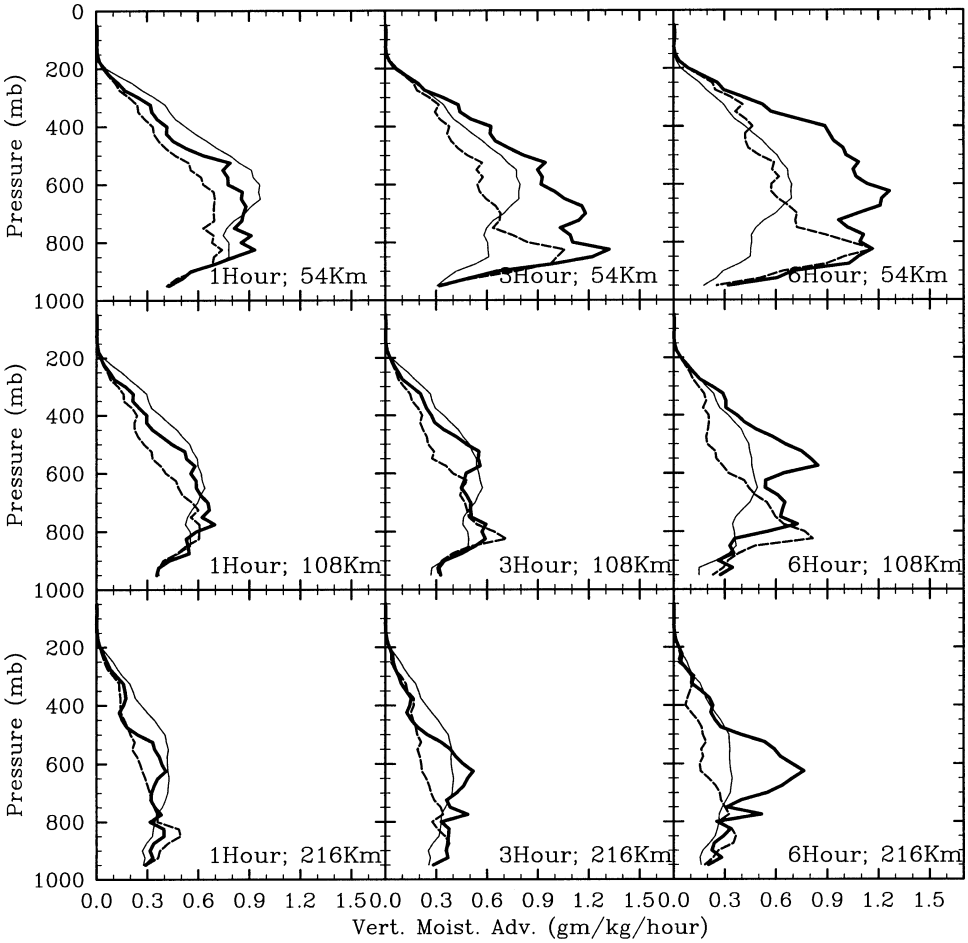

FIG. 9. Same as Fig. 8, except for diagnosed vertical advection of moisture.

parison of the analyzed horizontal moisture flux convergence from the model soundings and their associated errors relative to the model's true domain-averaged values based on the 1 August 1995 simulation using the five-sounding network from the upper-left 108-km grid (see Fig. 4) and 3-h sampling. The diagnosed vertical velocity for this same case is plotted in Fig. 5 in the same format. In contrast to the results for the vertical velocity field, the degree of improvement provided by the VOA is mixed with the general result that the error characteristics (lower-left and middle panels) are fairly similar for the VOA and reference analysis, except for hours 4–6 when the VOA looks to have noticeably improved the analysis. However, when considering the rms errors over the entire day, or all cases with the same sampling (i.e., Fig. 10), the error characteristics of the reference and VOA analyses are fairly similar.

A closer examination of the errors and associated adjustments for the sample at hours 4–6 helps demonstrate the reason for the above similarity. In the reference analysis, there are relatively large negative errors near 650 and 950 hPa, and relatively minor errors elsewhere, with the result that the analysis has too much moisture entering the column. While it would be preferable to only reduce the size of the two larger errors, the nature of the VOA is to produce the smallest adjustments possible to the observed variables [in terms of variance; Eq. (5)] to bring about conservation of moisture (as well as heat, mass, and momentum). The result is that the small adjustments made throughout the column end up influencing the moisture flux convergence profile somewhat uniformly, at least in terms of the sign, to bring about moisture conservation. In this particular case, the adjustments led to an increase in moisture flux convergence below about 600 hPa, with the magnitude of the change increasing with increasing pressure. This change resulted in a near complete removal of the negative moisture flux convergence error at 950 hPa, a minor reduction in the negative error at 650 hPa, and the introduction of a positive error at 750 hPa that was not previously in the analysis. While the above situation is not ideal, the outcome is consistent with the VOA framework in that the overall variance associated with the adjustments made is less than if the (necessarily larger) corrections were isolated to only the 650- and 950-hPa levels. Thus, beyond the constraints

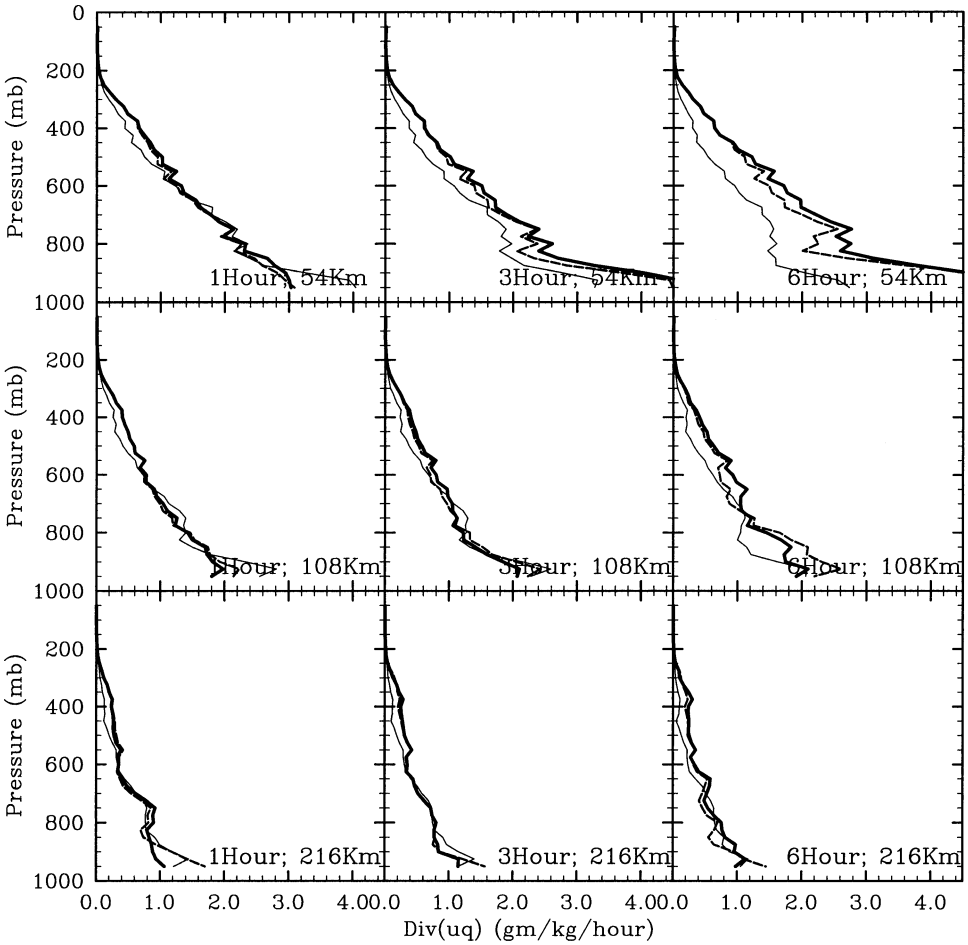

FIG. 10. Same as Fig. 8, except for diagnosed horizontal moisture flux convergence [$\nabla_H \cdot (\mathbf{V}_q)$].

associated with the vertical integrals, there is little constraining information to help determine which levels should be adjusted other than some overall bulk properties of the atmospheric column. For example, to change the amount of moisture convergence, small adjustments to the wind and moisture in the lower (moist) portion of the column would be expected to be more effective than adjustments in the upper (dry) portion of the column. Apart from the above limitation, which would seem inherent to the problem, it is worth reemphasizing that the VOA's utilization of the vertical constraints makes best use of the available information, which, as shown above, does translate into significant improvements in column integrated quantities, vertical velocity and vertical advective quantities that would not otherwise be forthcoming.

d. Additional sampling considerations

The present methodology provides the means to examine a number of additional sampling considerations. For example, what is the impact of using additional soundings on both the reference and VOA analyses? Figure 12 shows a comparison of the rms errors in diagnosed vertical velocity for both the reference analyses (green lines) and the VOA (red lines) for the cases of using five soundings (solid lines) and nine soundings (dotted lines) based on the sampling depicted in Fig. 4. For virtually every sampling condition applied, the added soundings improve the diagnosis. In general the benefits are more significant to the reference analyses than the VOA analyses. In fact, for the higher-frequency sampling (i.e., 1-h) and/or for the larger domain sizes, the differences between the reference analysis and VOA become considerably smaller, and the error characteristics for the two procedures are quite similar. In considering the error characteristics for the larger domain (i.e., 216 km) and 6-h sampling case, it is worth noting that for the most part the VOA with only five soundings performs at least as good as the reference analyses using nine soundings. Moreover, the VOA diagnosis appears to be less sensitive to the additional four soundings. This insensitivity is due, at least in part, to the VOA's incorporation of surface and TOA flux information during the period between the soundings.

An additional consideration that can be made with

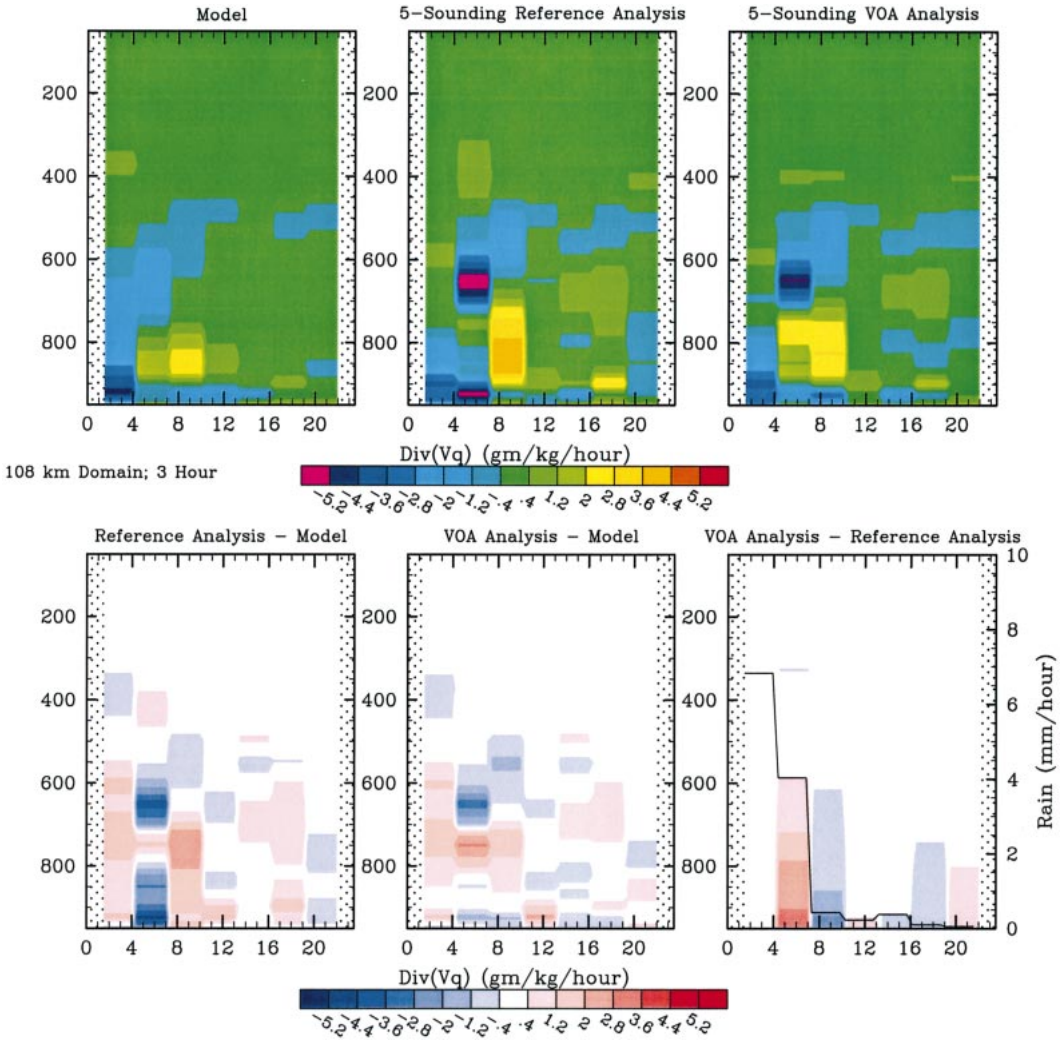

FIG. 11. Same as Fig. 5, except for diagnosed horizontal moisture flux convergence $[\nabla_H \cdot (\mathbf{V}_q)]$.

the present experimental framework is the impact that hydrometeor measurements might have on the VOA diagnosis. For the base case analyses, the storage term of water associated with hydrometeors in Eqs. (1) and (2) was set to zero. This was done because observations of such quantities have typically been unavailable, unreliable, and/or incomplete. However, since some progress is being made in this area through the use of satellite and cloud radars (e.g., Mace et al. 2001; Lazarus et al. 2000), it is worthwhile considering what impact these measurements might have on the accuracy of the diagnosis from the VOA. To examine this issue, all the analyses were computed again with the values for these terms prescribed from the model (i.e., from the cloud liquid water, snow, graupel, and rain components). In this case, it is presumed that these quantities can be measured and applied in the VOA in the same manner that precipitation can be measured and used as a constraint. It should be stressed that the results of this exercise would tend to provide an upper bound on the impact since the values used here are from the model and thus exact, and yet it is likely that significant uncertainties would exist in the measured values of these quantities.

The added impact from this additional hydrometeor information is demonstrated in Fig. 7. As discussed earlier, the red solid lines are the rms errors in vertical velocity for the VOA analysis without the inclusion of the hydrometeor information, while the red dotted lines incorporate the hydrometeor information as described above. The results show that the impact is mostly negligible, except for possibly the case of high-frequency sampling (e.g., 1 h) and relatively small domains (e.g., 54 or 108 km). Due to the small timescales and space scales associated with hydrometeor processes, their effects on the VOA become negligible for sampling times of 3 h or more, or a large spatial domain (e.g., 216 km). It should be stressed, however, that impacts from microphysical processes are expected only during disturbed periods for which phase changes in water are

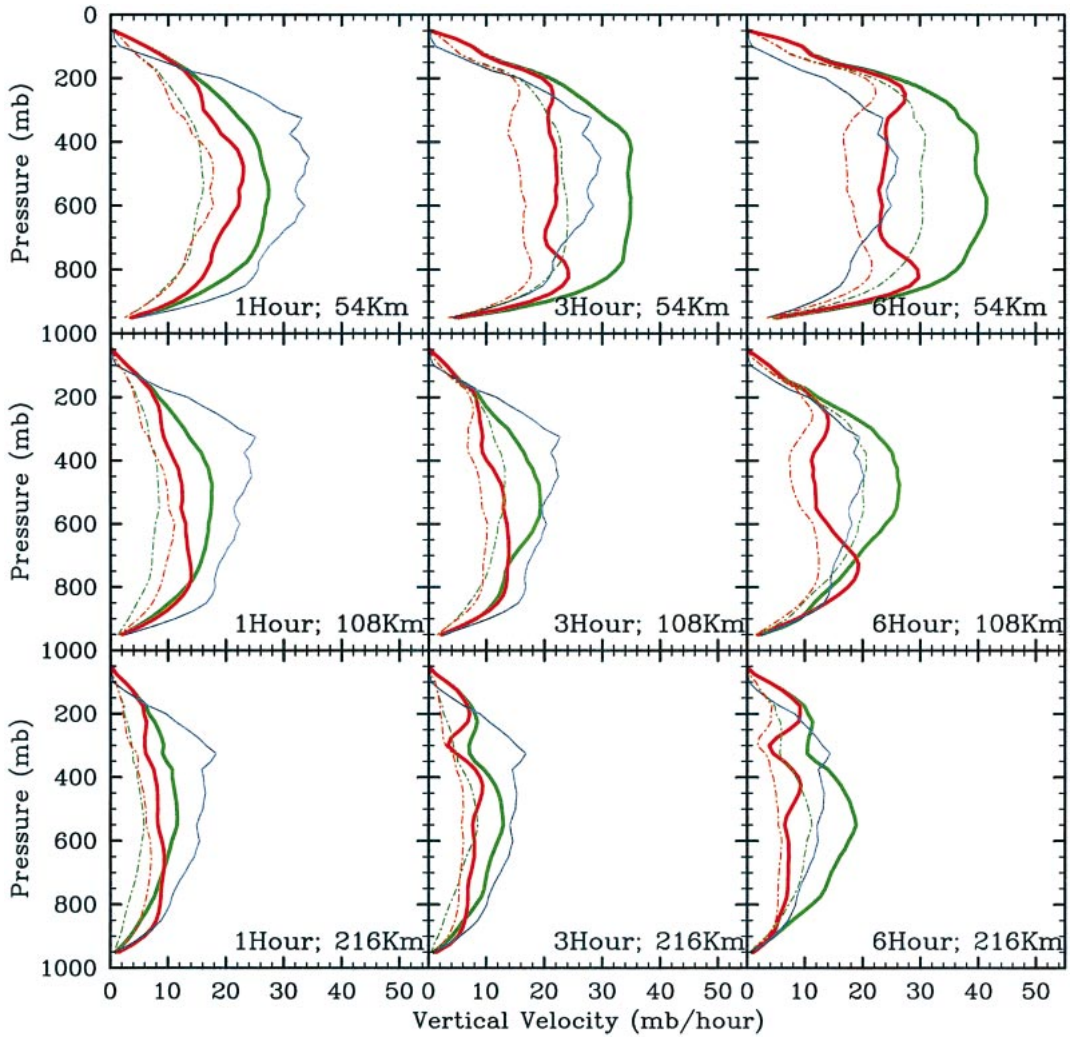

FIG. 12. Same as Fig. 7, except that the red (green) dotted lines show the rms differences between the VOA with all (mass only) constraints applied to nine model soundings (see Fig. 4) and the model's time- and domain-averaged values.

occurring. Thus, the above results that suggest a modest impact via the inclusion of hydrometeor information should be considered in light of the fact that they were derived from periods and domains that did in fact include a large fraction of undisturbed conditions when no impact could be expected. Thus, the comparison in Fig. 7 could be considered as the average impact of including hydrometeor information over four relatively disturbed 24-h periods, with each composed of both highly disturbed and undisturbed conditions (see Fig. 2).

Closer inspection of a given case illustrates a nontrivial improvement in the diagnosis that stems from the addition of hydrometeor information. Figure 13 shows results from the 20 July 1995 simulation for the northwest (i.e., upper left) 108-km domain and 1-h sampling. The upper-left panel shows the model time- and domain-averaged vertical velocity. In the early part of the simulation, there is a period of strong upward motion that corresponds to a significant rainfall (solid line in lower right). The lower-left panel shows that the lower atmosphere is moistening prior to this period of upward motion, drying out during the period of strong upward motion and heavy rainfall, and then moistening again after the rainfall subsides. The upper-middle panel shows the error in the diagnosed vertical velocity for the case when no hydrometeor information is provided to the VOA [as was the case for all the results described above (sections 5a–c)]. For this case, the VOA diagnosis significantly underestimates this upward motion, particularly in the lower portion of the atmosphere. Following this is a shorter period (simulation hour ~8–12), where the VOA overestimates the upward velocity. Examination of the hydrometeor budget of the model shows that there is a fairly significant amount of water vapor loss via the development of ice loading (i.e., cloud snow in this case) just prior to and during the period of heavy rainfall. Other hydrometeor components (e.g., graupel,

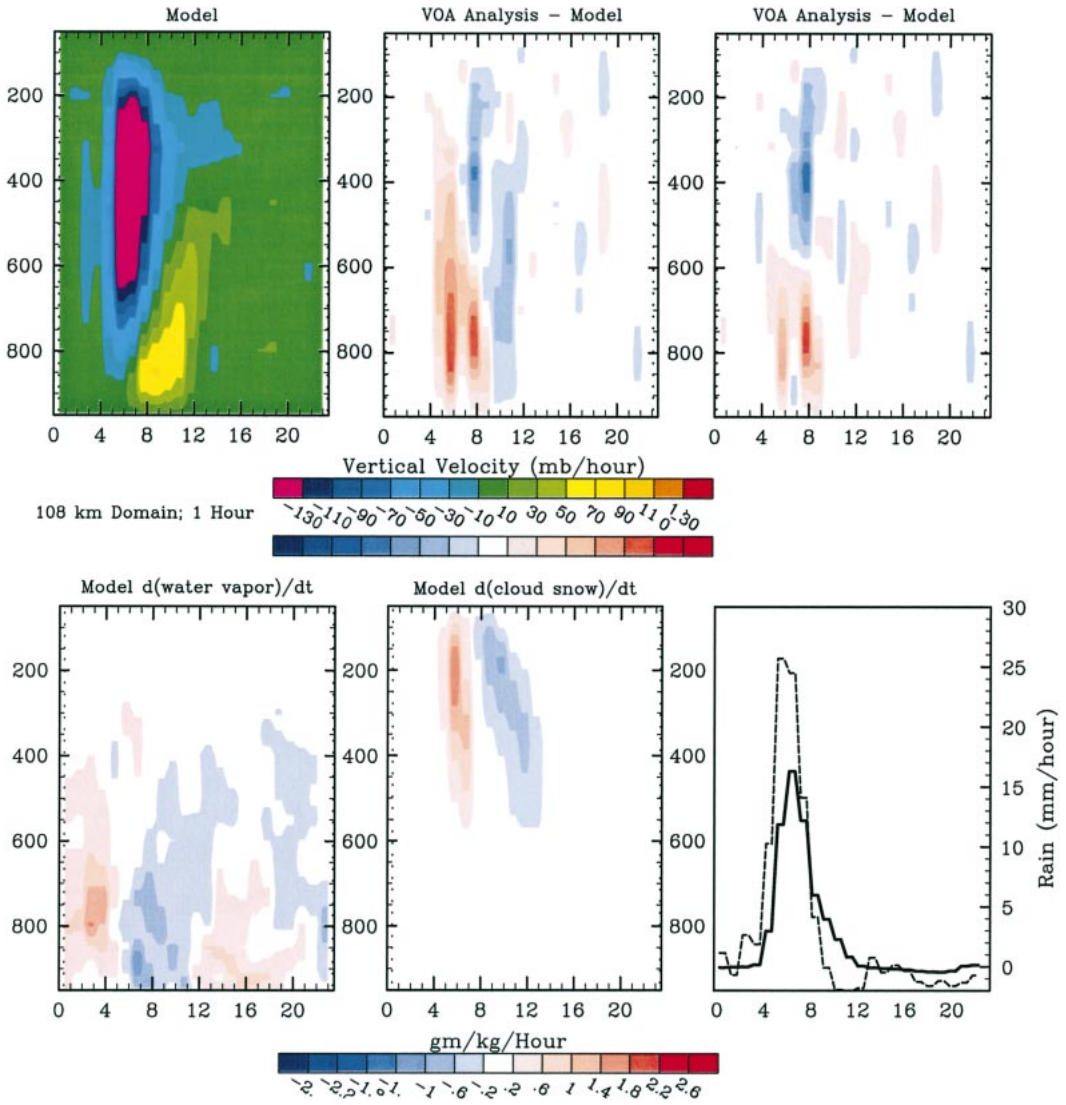

FIG. 13. Example of a case where the impact of hydrometeor information to the VOA improves the analysis (see section 5d); 20 Jul 1995, northwest intermediate size domain (i.e., upper-left 108-km box in Fig. 4) and 1-h sampling. (upper-left) Model time- and domain-averaged vertical velocity values. [upper-middle (right)] The analyzed vertical velocity values using the VOA with all constraints without (with) the addition of the hydrometeor information [i.e., last term in Eqs. (2) and (3)] as supplied from the model. [lower left (middle)] Time- and domain-averaged local time rate of change of water vapor (snow) from the model. (lower-right) The time- and domain-averaged precipitation (solid line) and the sum of the time- and domain-averaged precipitation and local time rate of change of water in hydrometeor form [dotted line; i.e., sum of the last two terms in Eq. (2)].

cloud rain) also grow, but the size of their sink in terms of water vapor is smaller and thus only the snow component is shown here (lower-middle panel). As the rainfall subsides the negative change in snow amount becomes a source of water vapor. Adding all the hydrometeor sinks and sources of water vapor [i.e., the last term in Eq. (2)] to the precipitation gives the dotted line in the lower-right panel. This dotted line can be thought of as an ''apparent'' precipitation. The upper-right panel shows the diagnosed vertical velocity errors when the hydrometeor information is included as a constraint on the VOA (as discussed above in reference to Fig. 7). Evident is the reduction in the underestimate of the upward vertical velocity just prior and during the rainfall event and a reduction in the overestimate of the upward vertical velocity after the rainfall event. These results suggest that under certain sampling and synoptic conditions (see discussion above), hydrometeor budget information may be valuable (cf. Petch and Dudia 1998).

As a final point worth considering it is worth noting that in addition to the fact that the atmosphere being examined here is a model representation, the model soundings do not contain any instrument error, and the surface and TOA flux terms do not contain any instrument or sampling error. To examine the impact that such errors might have on the VOA, idealized instrument

error was added to the model soundings and then the analyses were performed again using the base case conditions (e.g., five soundings and no hydrometeor information). The added error took the form of uncorrelated noise in both space and time. Specifically, random numbers scaled by the instrumental error (i.e., 0.2 K, 0.5 m s^{-1}, and 3% for water vapor; see ZET) were added to the temperature, wind, and water vapor sounding values. In addition, random errors of 30% were added to the model time- and domain-averaged rainfall and evaporation to account for observational uncertainty in these quantities (sampling and instrument errors). While detailed examination showed differences in the diagnosed quantities for both the reference and VOA analyses, overall the error characteristics were nearly identical to the base case analysis. For example, a plot such as Fig. 7 for the case with the above addition of errors is largely indistinguishable from the case where no additional error is added. This suggests that the bulk of the sampling error is made up of, or at least can be represented as, the spatial and temporal subsampling error of the observational array itself. This should not be taken to mean that other errors are not important in practice; it is just meant to indicate that for this study the lack of an instrument and/or subgrid-scale flux sampling error probably does not significantly alter the conclusions. One important difference between the idealized sampling errors added above and those occurring in practice are that often instrument biases are correlated in space or have systematic biases in terms of synoptic condition (e.g., temperature or moisture dependent). Moreover, drift of soundings with the environmental wind can also produce sampling errors (cf. ZET) that are not mimicked in any way by the idealized errors discussed above.

6. Summary and discussion

The objective of this study is to examine the effectiveness of the variational objective analysis (VOA) for producing realistic diagnoses of atmospheric field program data. A previous study (ZET) using observation data alone showed that analyzed results from the VOA were much less sensitive than more traditional methods of analysis to the amount and types of input data used in the analysis (e.g., Fig. 1). However, the underlying fact that the diagnosed quantities cannot be validated against the field observations themselves raises some questions regarding the actual accuracy of the VOA results, the level of improvement that is provided by the VOA over more conventional approaches, and the dependence of each of these considerations on sampling conditions and the amounts, types and uncertainties in the constraining data.

To address these questions, this study employed COAMPS cloud-resolving model simulations of atmospheric variability, and sampled the model output in a manner consistent with a typical field program using idealized sounding arrays. The simulations took the form of four separate 24-h forecasts for a region over the ARM Oklahoma CART site (see section 3; Fig. 3) during relatively disturbed periods during the ARM summer 1995 SGP IOP (Fig. 2). The model output and associated model soundings were then subject to a conventional form of analysis in which only a (variational form of) mass constraint was applied (referred to as the reference analysis) as well as to the complete VOA procedure (see sections 2 and 4). The diagnosed results from both analyses were then compared to time- and domain-averaged quantities from the model (i.e., ''truth''). This procedure provides the means to examine the accuracy of both methods of analysis and in turn assess the (expected) level of improvement of the VOA over the more conventional analyses. Moreover, it allows a way to test the sensitivity of the results to sampling timescales and space scales, sources of input data, synoptic condition, etc.

The assessments and comparisons were generally made using vertical velocity and advective tendencies of temperature and water vapor as diagnostic quantities. Assessments were made using nine different sampling conditions that include sampling arrays of 54, 108, and 216 km and temporal sampling of 1, 3, and 6 h (Fig. 4). The results showed that for diagnosed vertical velocity and vertical advective tendencies, the VOA values typically exhibited considerably smaller errors compared to the values from the reference analyses, with the level of improvement and overall accuracy being dependent on synoptic and sampling conditions (Figs. 5–9). Highly relevant is the finding that often the errors associated with the reference analyses have a magnitude similar to, or greater than, the variability of the field being diagnosed whereas the errors associated with the VOA are more often typically less than the variability of the field. In terms of the dependence of the errors on synoptic conditions, the improvements by the VOA tend to be greatest during disturbed conditions, with the errors typically being smaller and comparable between the two methods of analyses during undisturbed conditions. In terms of the dependence of the results on sampling conditions, the errors for both types of analyses increase as the spatial domain decreases, and for the most part decrease with more frequent temporal sampling. However, the improvement achieved by having more frequent sampling is rather modest for the VOA since it already incorporates time-mean surface and TOA fluxes as constraints, and thus indirectly incorporates some aspects of the variability between sampling times.

Practically speaking, the results concerning sampling dependence (specifically Figs. 7–9) suggest that large array spacing is advantageous (in that it the diagnosed quantities have the smallest absolute errors), and that 6-h sampling, as compared to more frequent sampling, may be adequate. This conclusion derives from the fact that 6-h sampling is considerably more economical and that the errors for the VOA analysis only marginally

improve in going from 6-h sampling to 1- or 3-h sampling. Of course this conclusion rests on the requirement that the VOA be employed for the analysis, and that adequate surface and TOA fluxes are available to constrain the VOA.

In contrast to the vertical velocity and advection terms, on average, virtually no level-by-level improvement by the VOA was found over the reference analysis in diagnosed moisture flux convergence, wind divergence, or horizontal advection tendencies. In addition, the errors in these terms were found to be as large as the variability of the field itself. These two results, particularly the former, are not entirely unexpected since the adjustments to horizontal wind, moisture, and temperature are relatively small. Moreover, given the nature of the (vertically integrated) constraints, there is little information that can be used to determine the levels at which adjustments should be made (i.e., errors are not necessarily uniform with height or small). Moreover, there is no integrated effect of the error and/or improvement in the error made for the horizontal advection quantities as is the case for the vertical advection terms via the diagnosis of the vertical velocity. Under the present observational and VOA framework, little can be done to improve this situation since the adjustments affecting these horizontal advection/convergence terms are inherently required to be small and as yet there are no obvious candidate observations that could provide useful constraints to help better dictate the height dependence of the adjustments.

The impact of adding additional soundings (nine instead of five; Fig. 4) showed that the improvements were typically more beneficial to the reference analyses than the VOA analyses, and in some cases allowed the error characteristics of the reference analysis to become similar to those of the VOA analysis. Noteworthy was the finding that the results from the VOA analyses using five soundings were often as good or better than the results from the reference analyses using nine soundings. These results could be interpreted as suggesting that application of the VOA can provide improvements to an observing system diagnosis that are somewhat akin to including additional soundings. However, it should be noted that the VOA does require additional measurements that the more traditional analyses do not require.

The impact that hydrometeor measurements would have in providing additional constraints on the VOA was also investigated by incorporating the sources/sinks of water vapor and temperature associated with phase changes of hydrometeors into the precipitation field that are used to constrain the VOA [Eqs. (2)–(3)]. The results showed that the impact is mostly negligible when averaging over relatively large space (i.e., $>\sim$100 km) or timescales (e.g., 6-h sampling). On the other hand, the results suggest that for frequent sampling (e.g., 1–3 h) and for rather small spatial scales (i.e., $<\sim$100 km), there is a definite favorable impact on the VOA results for highly disturbed periods. While this latter result is deemed reasonable, the determination of the exact scales at which hydrometeor information becomes valuable to the VOA application could be somewhat dependent on the model used in the assessment as well as on the synoptic condition. In any case, these results indicate that some noteworthy improvements in objectively analyzed data from the VOA might be possible given more improvements in technology and practices used to measure/derive hydrometeor information. As a corollary to this finding, Petch and Dudia (1998) show that the inclusion of hydrometeor advection tendencies in the large-scale forcing for SCM simulations can have a significant impact on the evolution of the model physics. Thus, whether the hydrometeor information is used to explicitly include hydrometeor advection in the large-scale forcing, or (as in the present study) is used as an additional constraint in the VOA, it appears that under certain circumstances this information can be valuable.

As a final remark, a study by Guichard et al. (2000) argued that before stringent evaluation can be made of the performance of physical parameterizations in model simulations (e.g., from SCM or CRM tests), it is necessary to obtain better insight into the uncertainties in the diagnosed advective tendencies used as large-scale forcing. The methodology presented here along with the varying levels of agreement between the analyses and model values provides some framework for estimating these uncertainties.

Acknowledgments. Support for this study was provided by the Office of Naval Research under Grants N00014-97-10527 (DW), through the Office of Naval Research, Program Element 0601153N (JR), the DOE ARM Program under Grant EFG0298ER62570 (MZ), and by NSF under Grant ATM901950 (MZ). Work at LLNL (SX) was performed under the auspices of the U. S. Department of Energy by the University of California, Lawrence Livermore National Laboratory under Contract W-7405-Eng-48. In addition, computational support was provided by a grant of computing time from the Department of Defense's High Performance Computing Program. This study's analysis and presentation benefited from the use of the NCAR Graphics Package and Seaspace Corporation's TeraScan software system.

REFERENCES

Carney, T. Q., and D. G. Vincent, 1986: Meso-synoptic scale interactions during AVE/SESAME 1, 10–11 April 1979. Part II: Influence of convective activity on larger scale flow. *Mon. Wea. Rev.*, **114,** 353–370.

Davies, H. C., 1976: A lateral boundary formulation for multi-level prediction models. *Quart. J. Roy. Meteor. Soc.*, **102,** 405–418.

Ferrier, B. S., 1988: One-dimensional time-dependent modeling of squall-line convection. Ph.D. thesis, University of Washington, 259 pp.

Ghan, S., and Coauthors, 2000: An intercomparison of single column model simulations of summertime midlatitude continental convection. *J. Geophys. Res.*, **105,** 2091–2124.

Guichard, F., J. L. Redelsperger, and J. P. Lafore, 2000: Cloud-resolving simulation of convective activity during TOGA COARE: Sensitivity to external sources of uncertainties. *Quart. J. Roy. Meteor. Soc.,* **126,** 3067–3095.

Gunn, B. W., J. L. McBride, G. J. Holland, T. D. Keenan, N. E. Davidson, and H. H. Hendon, 1989: The Australian summer monsoon circulation during AMEX Phase II. *Mon. Wea. Rev.,* **117,** 2554–2574.

Harshvardhan, R. Davies, D. Randall, and T. Corsetti, 1987: A fast radiation parameterization for atmospheric circulation models. *J. Geophys. Res.,* **92,** 1009–1015.

Hodur, R. M., 1997: The Naval Research Laboratory's Coupled Ocean/Atmosphere Mesoscale Prediction System (COAMPS). *Mon. Wea. Rev.,* **125,** 1414–1430.

Hogan, T. F., and T. E. Rosmond, 1991: The description of the U.S. Navy Operational Global Atmospheric Prediction System's spectral forecast model. *Mon. Wea. Rev.,* **119,** 1786–1815.

Holland, J. Z., and E. M. Rasmusson, 1973: Measurements of atmospheric mass, energy and momentum budgets over a 500-kilometer square of tropical ocean. *Mon. Wea. Rev.,* **101,** 44–55.

ISMGG (International and Scientific Management Group of GATE), 1974: GATE. *Bull. Amer. Meteor. Soc.,* **55,** 711–744.

Kain, J. S., and J. M. Fritsch, 1990: A one-dimensional entraining/detraining plume model and its application in convective parameterization. *J. Atmos. Sci.,* **47,** 2784–2802.

Kuo, Y.-H., and R. A. Anthes, 1984: Accuracy of diagnostic heat and moisture budgets using SESAME-79 field data as revealed by observing system simulation experiments. *Mon. Wea. Rev.,* **112,** 1465–1482.

Lazarus, S. M., S. K. Krueger, and G. G. Mace, 2000: A cloud climatology of the Southern Great Plains ARM CART. *J. Climate,* **13,** 1762–1775.

Lin, X., and R. H. Johnson, 1996: Heating, moistening, and rainfall over the western Pacific warm pool during TOGA COARE. *J. Atmos. Sci.,* **53,** 3367–3383.

Louis, J. F., M. Tiedtke, and J. F. Geleyn, 1982: A short history of the operational PBL-parameterization at ECMWF. *Proc. Workshop on Planetary Boundary Parameterization,* Reading, United Kingdom, ECMWF, 59–79.

Mace, G. G., and T. P. Ackerman, 1996: Assessment of error in synoptic scale diagnostics derived from wind profiler and radiosonde network data. *Mon. Wea. Rev.,* **124,** 1521–1534.

——, E. E. Clothiaux, and T. P. Ackerman, 2001: The composite characteristics of cirrus clouds: Bulk properties revealed by one year of continuous cloud radar data. *J. Climate,* **14,** 2185–2203.

Mellor, G., and T. Yamada, 1974: A hierarchy of turbulence closure models for planetary boundary layers. *J. Atmos. Sci.,* **31,** 1791–1806.

Nitta, T., and S. Esbensen, 1974: Heat and moisture budget analyses using BOMEX data. *Mon. Wea. Rev.,* **102,** 17–28.

O'Brien, J. J., 1970: Alternative solutions to the classical vertical velocity problem. *J. Appl. Meteor.,* **9,** 197–203.

Ooyama, K., 1987: Scale-controlled objective analysis. *Mon. Wea. Rev.,* **115,** 2476–2506.

Petch, J. C., and J. Dudhia, 1998: The importance of horizontal advection of hydrometeors in a single column model. *J. Climate,* **11,** 2437–2452.

Randall, D. A., K. M. Xu, R. C. J. Somerville, and S. Iacobellis, 1996: Single-column models and cloud ensemble models as links between observations and climate models. *J. Climate,* **9,** 1683–1697.

Rutledge, S. A., and P. V. Hobbs, 1983: The mesoscale and microscale structure of organization of clouds and precipitation in midlatitude cyclones. VIII: A model for the ''seeder–feeder'' process in warm-frontal rainbands. *J. Atmos. Sci.,* **40,** 1185–1206.

Slingo, J. M., 1987: The development and verification of a cloud prediction scheme for the ECMWF model. *Quart. J. Roy. Meteor. Soc.,* **113,** 899–927.

Stokes, G. M., and S. E. Schwartz, 1994: The Atmospheric Radiation Measurement (ARM) program: Programmatic background and design of the cloud and radiation test bed. *Bull. Amer. Meteor. Soc.,* **75,** 1201–1221.

Webster, P. J., and R. Lukas, 1992: TOGA COARE: The Coupled Ocean–Atmosphere Response Experiment. *Bull. Amer. Meteor. Soc.,* **73,** 1377–1416.

Weisman, M. L., W. C. Skamarock, and J. B. Klemp, 1997: The resolution dependence of explicitly modeled convective systems. *Mon. Wea. Rev.,* **125,** 527–548.

Zhang, M. H., and J. L. Lin, 1997: Constrained variational analysis of sounding data based on column-integrated budgets of mass, heat, moisture, and momentum: Approach and application to ARM measurements. *J. Atmos. Sci.,* **54,** 1503–1524.

——, J. L. Lin, R. T. Cederwall, J. J. Yio, and S. C. Xie, 2001a: Objective analysis of the ARM IOP data: Method and sensitivity. *Mon. Wea. Rev.,* **129,** 295–311.

——, S. Xie, R. T. Cederwall, and J. J. Yio, 2001b: Description of the ARM Operational Objective Analysis System. ARM Tech. Rep. 005, 19 pp.